

Identity-Free Facial Expression Recognition using conditional Generative Adversarial Network

Jie Cai¹, Zibo Meng², Ahmed Shehab Khan¹, Zhiyuan Li¹, James O'Reilly¹, and Yan Tong¹

¹Department of Computer Science & Engineering, University of South Carolina, Columbia, SC

²Innopeak Technology Inc., Palo Alto, CA

{jcai,akhan,zhiyuanl,oreillyj}@email.sc.edu, mzbo1986@gmail.com, tongy@cec.sc.edu

Abstract

In this paper, we proposed a novel Identity-free conditional Generative Adversarial Network (IF-GAN) to explicitly reduce inter-subject variations for facial expression recognition. Specifically, for any given input face image, a conditional generative model was developed to transform an average neutral face, which is calculated from various subjects showing neutral expressions, to an average expressive face with the same expression as the input image. Since the transformed images have the same synthetic “average” identity, they differ from each other by only their expressions and thus, can be used for identity-free expression classification. In this work, an end-to-end system was developed to perform expression transformation and expression recognition in the IF-GAN framework. Experimental results on three facial expression datasets have demonstrated that the proposed IF-GAN outperforms the baseline CNN model and achieves comparable or better performance compared with the state-of-the-art methods for facial expression recognition.

1 INTRODUCTION

Facial expression is a natural and universal means for human communication and has been extensively studied over the past decades. Most recently, Convolutional Neural Networks (CNNs) have achieved promising results on facial expression recognition. However, most of the existing approaches were optimized using all subjects from training data, while high inter-subject variations caused by individual differences in facial attributes are not explicitly considered. As a result, the learned features may capture more identity-related information than expression-related information, as discussed in [1], and are not purely related to the specific task, i.e., facial expression recognition. Therefore, performance of facial expression recognition usually degrades for unseen subjects.

This motivates us to reduce the effects of identity-related variations by explicitly removing the identity information from face images. Specifically, let $f(\mathbf{I})$ be the extracted facial representation of an input image \mathbf{I} learned by CNNs. $f(\mathbf{I})$ is usually a result of a nonlinear function of two kinds of features, i.e. $f(\mathbf{I}) = g(f_{id}(\mathbf{I}), f_{exp}(\mathbf{I}))$, where $f_{id}(\mathbf{I})$ represents the identity-

related features affected by gender, age, race, etc.; and $f_{exp}(\mathbf{I})$ represents the expression-related information. The objective of facial expression recognition is to make the best use of $f_{exp}(\mathbf{I})$ while minimizing the influence of $f_{id}(\mathbf{I})$. To achieve this goal, we proposed a novel Identity-free conditional Generative Adversarial Network (IF-GAN), as shown in Fig. 1, to remove the identity information by transferring the expression information from the input image to a synthetic identity, i.e., an “average” face calculated from all subjects in the dataset. Such generated images have the same synthetic “average” identity and differ from each other by only expressions. Hence, these “average” expressive images will be used for identity-free expression classification.

In summary, our major contributions are:

- Developing a novel IF-GAN model to transfer an expression of an arbitrary subject to a synthetic “average” identity for identity-free expression recognition; and
- Developing an end-to-end system to perform expression synthesis and expression recognition simultaneously.

Extensive experiments on three facial expression datasets have shown that the proposed IF-GAN yields considerable improvement over the baseline CNN by generating and employing identity-free face images for expression recognition. The IF-GAN also achieves comparable or better performance compared to the state-of-the-art methods.

2 RELATED WORK

Facial expression recognition has been widely studied in the past decades as detailed in the recent surveys [7, 8, 9]. One of the major steps is to capture the most discriminative features that characterize appearance and geometric facial changes caused by target expressions. These features can be roughly divided into two main categories: human-designed and learned features. Recently, deep CNNs have achieved promising results for facial expression recognition [9]. However, the learned expression-related deep features are often affected by individual differences in facial attributes affected by gender, race, age, etc. As a result, performance of expression recognition usually degrades on unseen subjects. Although great progress has been achieved in feature/classifier selections, the challenge caused by inter-subject variations still remains for facial expression recognition.

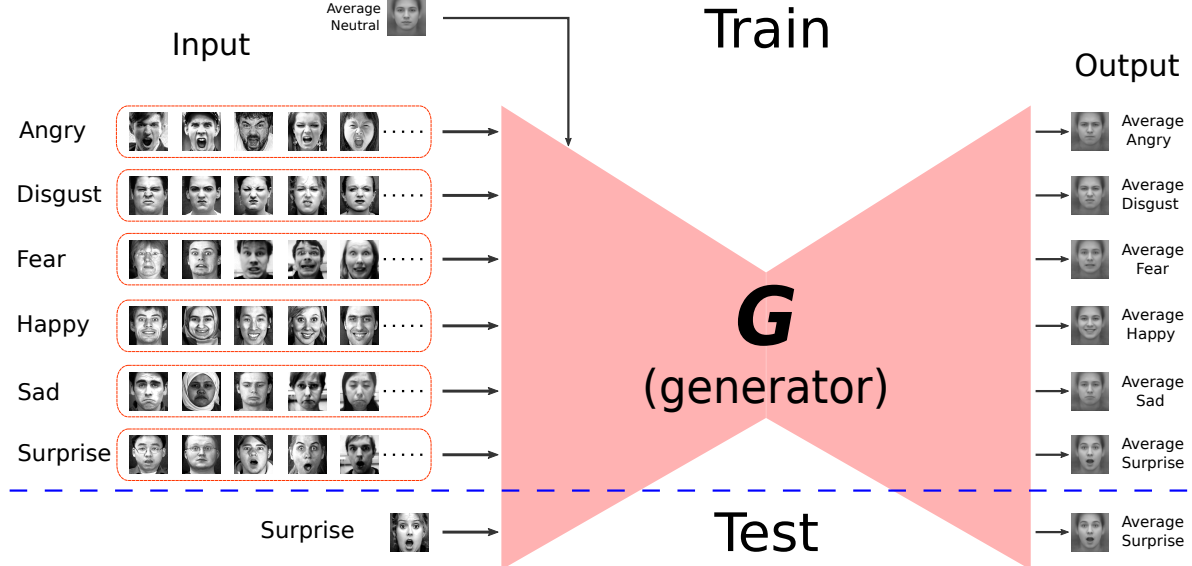


Figure 1: An illustration of the IF-GAN synthesizing identity-free expressive faces from input images. Best viewed in color.

Approaches [3, 4] were designed to learn discriminative features for facial expression recognition by reducing the intra-class variations while increasing the inter-class differences simultaneously. More recently, there are a few approaches focusing on explicitly improving person-independent facial expression recognition. An Identity-Aware CNN (IACNN) [2] was proposed to alleviate variations introduced by identity-related information using an expression-sensitive contrastive loss and an identity-sensitive contrastive loss. However, the contrastive loss suffers from drastic data expansion when constructing image pairs from the training data. An Identity-Adaptive Generation (IA-gen) method [1] was developed to generate person-dependent facial expression images such that any given input facial image is transferred to six expressive images of the same subject using six conditional GANs (cGANs). Then, expression classification is performed by comparing the input image with the six generated expressive images. De-expression Residue Learning (DeRL) [10] also utilized the cGAN to synthesize a neutral facial image of the same identity from any input expressive image, while the person-independent expression information can be extracted from the intermediate layers of the generative model. However, the aforementioned cGAN-based models [1, 10] are not end-to-end networks and suffer from expensive computational cost.

3 METHODOLOGY

3.1 A Brief Review of Generative Adversarial Networks

Traditional Generative Adversarial Networks (GANs) [5] are deep neural architectures used to generate realistic images by implementing a system with two networks involved: a generator, \mathbf{G} , and a discriminator, \mathbf{D} . Specifically, a generator is trained to capture the underlying distribution of the training data, while a dis-

criminator is trained to estimate the probability of a sample coming from the real distribution p_y or the generator. The objective of the GAN is to train a \mathbf{D} that identifies fake samples generated by \mathbf{G} from samples drawn from the true distribution, while encouraging \mathbf{G} to generate realistic samples to deceive \mathbf{D} . GANs are optimized with the following objective function:

$$\min_{\mathbf{G}} \max_{\mathbf{D}} V(\mathbf{D}, \mathbf{G}) = \mathbb{E}[\log(\mathbf{D}(\mathbf{y}))] + \mathbb{E}[\log(1 - \mathbf{D}(\mathbf{G}(\mathbf{z})))] \quad (1)$$

where \mathbf{y} is a real sample from the true data distribution and \mathbf{z} is a random noise vector drawn from a distribution p_z .

In contrast to traditional GANs that learn a mapping from the random noise vector \mathbf{z} to a target sample \mathbf{y} , i.e., $\mathbf{G}(\mathbf{z}) \rightarrow \mathbf{y}$, conditional GANs (cGANs) [6] learn a mapping from a random noise vector \mathbf{z} to the target \mathbf{y} conditioned on an observed signal \mathbf{x} , i.e., $\mathbf{G}(\mathbf{x}, \mathbf{z}) \rightarrow \mathbf{y}$. cGAN are optimized with the following value function:

$$\begin{aligned} \min_{\mathbf{G}} \max_{\mathbf{D}} V(\mathbf{D}, \mathbf{G}) = & \mathbb{E}[\log(\mathbf{D}(\mathbf{x}, \mathbf{y}))] \\ & + \mathbb{E}[\log(1 - \mathbf{D}(\mathbf{x}, \mathbf{G}(\mathbf{x}, \mathbf{z})))] \end{aligned} \quad (2)$$

3.2 The Proposed IF-GAN Architecture

The objective of the proposed IF-GAN is to transfer the expression information from the input image to a synthetic “average” identity; and then the generated “average” expressive image will be used for identify-free expression classification. Given an input image \mathbf{I} , the extracted facial features $f(\mathbf{I})$ can be represented by two kinds of features $f_{id}(\mathbf{I})$, i.e., identity-related features, and $f_{exp}(\mathbf{I})$, i.e., expression-related features, which are nonlinearly coupled with each other. Let \mathbf{I}_{SE} be a face image of any real subject associated with a specific expression, \mathbf{I}_{AN} be a face image of a synthetic “average” subject with a neutral expression, which is

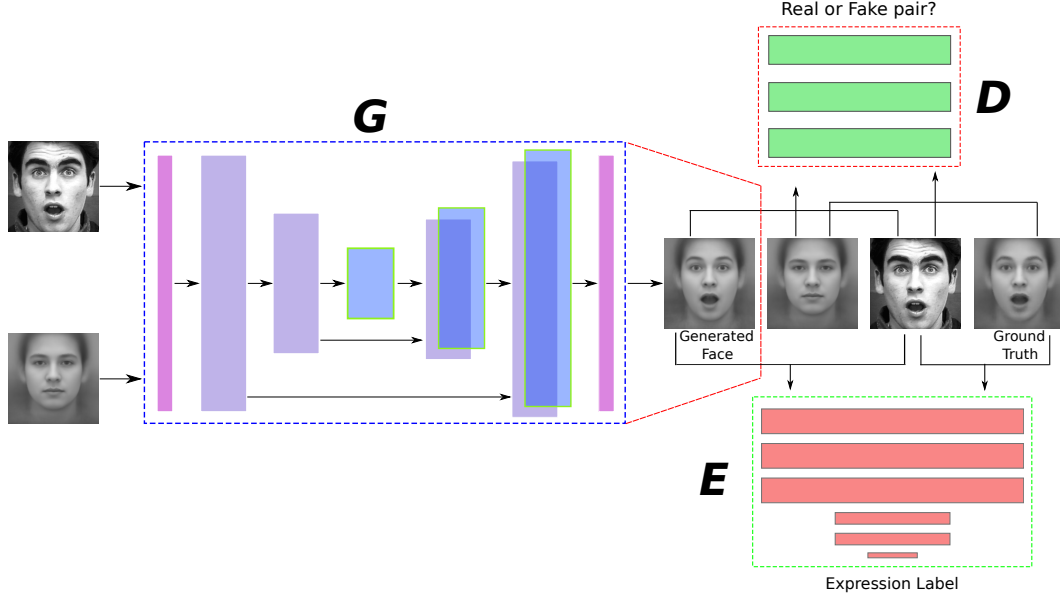


Figure 2: A complete architecture of the IF-GAN consists of three models: (1) a generator (**G**) which is a “U-Net” [11] with skip connections between mirrored layers in the encoder and decoder stacks, (2) a discriminator (**D**) which is a “PatchGAN” that only penalizes structure at the scale of patches, and (3) the expression classifier (**E**) which is a ResNet-34 network pre-trained on the ImageNet dataset.

calculated as the average of all subjects showing a neutral expression in the dataset, and \mathbf{I}_{AE} be the target expressive face image of the “average” subject calculated from all subjects showing the specific expression in the dataset. A generator (**G**) is developed to transfer the expression information $f_{exp}(\mathbf{I}_{SE})$ from the image \mathbf{I}_{SE} to the “average” subject such that a synthetic expressive face image $\tilde{\mathbf{I}}_{AE}$ of the “average” subject is generated with the same expression as \mathbf{I}_{SE} . In contrast to the regular GANs or cGANs, an expression classifier (**E**) is employed to ensure the generated “average” expressive image ($\tilde{\mathbf{I}}_{AE}$) has the same expression as the input image \mathbf{I}_{SE} .

As shown in Fig. 2, the proposed IF-GAN contains three networks, i.e., a generator (**G**), a discriminator (**D**), and an expression classifier (**E**). The generator takes a pair of images, i.e. $\{\mathbf{I}_{AN}, \mathbf{I}_{SE}\}$, as input; and generates an expressive face image $\tilde{\mathbf{I}}_{AE}$ of the “average” subject. Then, the fake tuple $\{\mathbf{I}_{AN}, \mathbf{I}_{SE}, \tilde{\mathbf{I}}_{AE}, 0\}$ and the real tuple $\{\mathbf{I}_{AN}, \mathbf{I}_{SE}, \mathbf{I}_{AE}, 1\}$ are fed into the discriminator for fake/real classification. Finally, $\{\mathbf{I}_{SE}, \mathbf{I}_{AE}, l_e\}$ and $\{\mathbf{I}_{SE}, \tilde{\mathbf{I}}_{AE}, l_e\}$, where l_e is the corresponding expression label, are utilized to fine-tune the expression classifier.

In this work, we used a “U-Net”-based architecture [12] for the generator, a convolutional “PatchGAN” classifier [13], which only penalizes structure at image level, for the discriminator, and a ResNet-34 [14] for the expression classifier. In contrast to DeRL [10] and IA-gen [1], **G**, **D** and **E** are jointly optimized during the IF-GAN training. Note that only **G** and **E** are employed during testing.

3.3 Loss Function of IF-GAN

The overall loss function of IF-GAN is defined as:

$$\mathcal{L} = \lambda_1 \cdot \mathcal{L}_{cGAN}(\mathbf{G}, \mathbf{D}) + \lambda_2 \cdot \mathcal{L}_{L1}(\mathbf{G}) + \lambda_3 \cdot \mathcal{L}_{softmax}(\mathbf{E}) \quad (3)$$

where the hyperparameters λ_1 , λ_2 , and λ_3 ¹ are used to balance the three terms.

The first term of Eq. 3 is the loss function of a cGAN and defined as:

$$\begin{aligned} \mathcal{L}_{cGAN}(\mathbf{G}, \mathbf{D}) = & \mathbb{E}[\log(\mathbf{D}(\{\mathbf{I}_{AN}, \mathbf{I}_{SE}, \mathbf{I}_{AE}\})))] \\ & + \mathbb{E}[\log(1 - \mathbf{D}(\{\mathbf{I}_{AN}, \mathbf{I}_{SE}, \mathbf{G}(\{\mathbf{I}_{AN}, \mathbf{I}_{SE}\})\}))] \end{aligned} \quad (4)$$

where $\{\mathbf{I}_{AN}, \mathbf{I}_{SE}, \mathbf{G}(\{\mathbf{I}_{AN}, \mathbf{I}_{SE}\})\}$ denotes the fake tuple, $\{\mathbf{I}_{AN}, \mathbf{I}_{SE}, \mathbf{I}_{AE}\}$ denotes the real tuple, and $\mathbf{G}(\{\mathbf{I}_{AN}, \mathbf{I}_{SE}\})$ is the generated image $\tilde{\mathbf{I}}_{AE}$. To compete against **D**, $\mathbf{G}(\cdot)$ learns to capture the true data distribution to generate realistic images that are similar to the images sampled from the true data distribution. We explore this option using $L1$ distance:

$$\mathcal{L}_{L1}(\mathbf{G}) = \mathbb{E}[\|\mathbf{I}_{AE} - \mathbf{G}(\{\mathbf{I}_{AN}, \mathbf{I}_{SE}\})\|_1] \quad (5)$$

Therefore, **G** tries to minimize this loss and compete against **D** that tries to maximize it, i.e.,

$$\mathbf{G}^* = \arg \min_{\mathbf{G}} \max_{\mathbf{D}} \lambda_1 \cdot \mathcal{L}_{cGAN}(\mathbf{G}, \mathbf{D}) + \lambda_2 \cdot \mathcal{L}_{L1}(\mathbf{G}) \quad (6)$$

Furthermore, **E** is jointly trained with **D** and **G**. Employing a softmax loss, the expression loss is defined as:

$$\begin{aligned} \mathcal{L}_{softmax}(\mathbf{E}) = & \mathbb{E}[\log p(l_e | \{\mathbf{I}_{SE}, \mathbf{I}_{AE}\})] \\ & + \mathbb{E}[\log p(l_e | \{\mathbf{I}_{SE}, \mathbf{G}(\{\mathbf{I}_{AN}, \mathbf{I}_{SE}\})\})] \end{aligned} \quad (7)$$

¹In our experiments, we set $\lambda_1 = 1$, $\lambda_2 = 200$, and $\lambda_3 = 50$ empirically.

4 EXPERIMENTS

To illustrate the effectiveness of the proposed IF-GAN, extensive experiments have been conducted on three benchmark datasets, i.e., the BU-3DFE [15], the CK+ dataset [17, 18], and the MMI dataset [19].

4.1 Preprocessing

To reduce the in-plane rotation and scaling variations, face alignment was employed based on three facial keypoints, i.e., centers of two eyes and tip of nose. In addition, histogram equalization was utilized to reduce the effect of illumination changes. For data augmentation purposes, the processed facial images were resized to $N \times N$ with random horizontal flipping and a random rotation between -3° and 3° . $M \times M$ patches were randomly cropped as the input during training process and center cropped during testing. In our experiment, $\{N, M\}$ is set to $\{256, 224\}$ and $\{286, 256\}$ for the baseline CNN model and the proposed IF-GAN, respectively. For the proposed IF-GAN, \mathbf{I}_{SE} , $\mathbf{\tilde{I}}_{AE}$ and \mathbf{I}_{AE} were further resized to 224×224 before being fed into \mathbf{E} for facial expression recognition.

4.2 Experimental Datasets

BU-3DFE dataset consists of 2,500 pairs of 3D static facial models and 2D facial images from 100 subjects of different races and ages. Each subject displays six basic expressions with four intensity levels and a neutral expression. Following [1, 10], we employed 1,200 images containing the 2D texture images of the six basic expressions with high intensity, i.e., the last two levels, in our experiment.

CK+ dataset includes 327 videos collected from 118 subjects, each of which is labeled with one of seven expressions, i.e., contempt and six basic expressions. Each video starts with a neutral face, and reaches the peak in the last frame. The last three frames from 309 videos labeled as one of the six basic expressions were collected with the labeled expression. Hence, an experimental dataset including 927 images was built for six basic expressions.

MMI dataset contains 236 sequences from 32 subjects, from which 208 sequences of 31 subjects displaying six basic expressions captured in frontal-view were selected in our experiments. Each video starts from a neutral expression, goes through a peak phase near the middle, and ends with a neutral face. Since the actual location of the peak frame was not provided, three frames in the middle of each sequence were collected as peak frames associated with the provided label, resulting in a total of 624 images for our experiments.

Training/testing strategy: In order to obtain more subtle facial expression data, the 50% images during the peak phase of CK+ and MMI sequences were used to construct training set for the baseline CNN and the proposed IF-GAN. Note that only the three peak frames in the CK+ and MMI sequences were used in testing.

A 10-fold cross-validation strategy was employed for all of the three datasets, where each dataset was split into 10 subsets and the subjects in any two subsets are mutually exclusive. For each run,

data from 8 sets were used for training, the remaining two subsets were used for validation and testing, respectively. The results were reported as the average of the 10 runs on the testing sets in terms of accuracy.

4.3 Implementation Details

Following [1, 10], the generator \mathbf{G} and discriminator \mathbf{D} were pre-trained on the BU-4DFE [20] dataset, where the middle 60% of images from the sequence were used. In addition, a ResNet-34 [14] network, which first pre-trained on the ImageNet dataset [12] and then further pre-trained on the BU-4DFE dataset, was employed as our baseline CNN model and the expression classifier (\mathbf{E}) in the proposed IF-GAN.

For evaluation on each dataset, the baseline ResNet-34 and IF-GAN were fine-tuned using their own training set, respectively, as well as the other two datasets as additional training data. Specifically, we employed 50% images from its own training set in every mini-batch. For each run of the 10-fold evaluation, the six average expressive face images \mathbf{I}_{AE} were obtained by averaging peak expressive images with the corresponding labels in the training set, respectively.

4.4 Experimental Results

Table 1: Performance comparison on the three facial expression datasets.

Method	Feature	BU-3DFE	CK+	MMI
Wang et al. [22]	3D-Static	61.79	–	–
Berretti et al. [23]	3D-Static	77.54	–	–
Yang et al. [24]	3D-Static	84.80	–	–
3DCNN [25]	Dynamic	–	85.9	53.2
ITBN [26]	Dynamic	–	86.3	59.7
F-Bases [27]	Dynamic	–	89.01	73.66
TMS [28]	Dynamic	–	91.89	–
Cov3D [29]	Dynamic	–	92.3	–
3DCNN-DAP [25]	Dynamic	–	92.4	63.4
STM-ExpLet [30]	Dynamic	–	94.19	75.12
LOMo [31]	Dynamic	–	95.1	–
STM [32]	Dynamic	–	96.40	–
DTAGN [33]	Dynamic	–	97.25	70.24
Lai et al. [34]	2D-Static	74.25	–	–
Zhang et al. [35]	2D-Static	80.95	–	–
MSR [36]	2D-Static	–	91.4	–
Center Loss [37]	2D-Static	–	92.25	73.40
Island Loss [4]	2D-Static	–	94.39	74.68
F-Bases [27]	2D-Static	–	94.81	57.56
IACNN [2]	2D-Static	–	95.37	71.55
DLP-CNN [3]	2D-Static	–	95.78	–
FN2EN [38]	2D-Static	–	96.80	–
IA-gen [1]	2D-Static	76.83	96.57	–
Lopes et al. [39]	2D-Static	72.89	96.76	–
PPDN [40]	2D-Static	–	97.3	–
DeRL [10]	2D-Static	84.17	97.3	73.23
ResNet-34	2D-Static	82.83	93.85	71.31
IF-GAN	2D-Static	84.25	95.90	74.52

As illustrated in Table 1, the proposed IF-GAN outperforms

the baseline ResNet-34 and achieves better or at least comparable results compared with the state-of-the-art methods on all the three datasets. Note that while most of the state-of-the-art methods take advantage of temporal information extracted from image sequences, the proposed IF-GAN is based on static frames, which is more favorable for applications with single images. For the BU-3DFE dataset, the proposed IF-GAN achieved the best performance under “2D-Static” setting without employing geometric features of the 3D shape model as Yang et al. [24] did, who achieved the best performance on the BU-3DFE dataset. For the CK+ dataset, although it achieves the best performance, DeRL [10] is not an end-to-end framework and requires high computational cost. Moreover, PPDN has the best performance on the CK+ dataset owing to the utilization of neutral images of the same subjects as reference. For the MMI dataset, Island Loss [4] achieved the best performance under “2D-Static” setting by taking the mean of the decision scores of the three peak images from the same sequence, while the proposed IF-GAN makes decisions based on a single image.

4.5 Expression Transfer Results

Fig. 3 shows several examples of the generated average expressive face images along with their corresponding input images on the BU-3DFE, CK+, and MMI datasets, respectively. As shown in Fig. 3, the generated face images totally removed the identity information from their corresponding input images, while the expression information is transferred to the “average” subject.

5 CONCLUSION

In this work, we proposed a novel end-to-end IF-GAN framework to perform identity-free expression recognition by generating expressive faces for a synthetic “average” subject. Our work differs from the other subject-independent methods in that the proposed IF-GAN is capable of removing subject-related information completely. Experimental results on three benchmark facial expression datasets have shown that the proposed IF-GAN achieves state-of-the-art recognition performance for facial expression recognition. For future work, we plan to apply our method for facial expression recognition in the wild to further deal with challenges introduced by large head movements.

6 ACKNOWLEDGEMENT

This work is supported by National Science Foundation under CAREER Award IIS-1149787. The Titan Xp used for this research was donated by the NVIDIA Corporation.

References

- [1] H. Yang, Z. Zhang, and L. Yin, “Identity-adaptive facial expression recognition through expression regeneration using conditional generative adversarial networks,” in *FG*. IEEE, 2018, pp. 294–301.
- [2] Z. Meng, P. Liu, J. Cai, S. Han, and Y. Tong, “Identity-aware convolutional neural network for facial expression recognition,” in *FG*. IEEE, 2017, pp. 558–565.
- [3] S. Li, W. Deng, and J. Du, “Reliable crowdsourcing and deep locality-preserving learning for expression recognition in the wild,” in *CVPR*, July 2017.
- [4] J. Cai, Z. Meng, A. Khan, Z. Li, J. O'Reilly, and Y. Tong, “Island loss for learning discriminative features in facial expression recognition,” in *FG*. IEEE, 2018, pp. 302–309.
- [5] I. Goodfellow, J. Pouget-Abadie, J. Mirza, B. Xu, D. Warde-Farley, S. Ozair, A. Courville, and Y. Bengio, “Generative adversarial nets,” in *NIPS*, 2014, pp. 2672–2680.
- [6] M. Mirza and S. Osindero, “Conditional generative adversarial nets,” *arXiv preprint arXiv:1411.1784*, 2014.
- [7] E. Sariyanidi, H. Gunes, and A. Cavallaro, “Automatic analysis of facial affect: A survey of registration, representation and recognition,” *IEEE T-PAMI*, vol. 37, no. 6, pp. 1113–1133, 2015.
- [8] B. Martinez, M. F. Valstar, B. Jiang, and M. Pantic, “Automatic analysis of facial actions: A survey,” *IEEE Trans. on Affective Computing*, vol. 13, no. 9, pp. 1–22, 2017.
- [9] S. Li and W. Deng, “Deep facial expression recognition: A survey,” *arXiv preprint arXiv:1804.08348*, 2018.
- [10] H. Yang, U. Ciftci, and L. Yin, “Facial expression recognition by de-expression residue learning,” in *CVPR*, 2018, pp. 2168–2177.
- [11] O. Ronneberger, P. Fischer, and T. Brox, “U-net: Convolutional networks for biomedical image segmentation,” in *MICCAI*. Springer, 2015, pp. 234–241.
- [12] O. Russakovsky, J. Deng, H. Su, J. Krause, S. Satheesh, S. Ma, Z. Huang, A. Karpathy, A. Khosla, M. Bernstein, et al., “Imagenet large scale visual recognition challenge,” *IJCV*, vol. 115, no. 3, pp. 211–252, 2015.
- [13] P. Isola, J. Zhu, T. Zhou, and A. A. Efros, “Image-to-image translation with conditional adversarial networks,” in *CVPR*, 2017.
- [14] K. He, X. Zhang, S. Ren, and J. Sun, “Deep residual learning for image recognition,” in *CVPR*, 2016, pp. 770–778.
- [15] L. Yin, X. Wei, Y. Sun, J. Wang, and M. Rosato, “A 3d facial expression database for facial behavior research,” in *FG*. IEEE, 2006, pp. 211–216.
- [16] G. Zhao, X. Huang, M. Taini, S. Li, and M. Pietikäinen, “Facial expression recognition from near-infrared videos,” *J. IVC*, vol. 29, no. 9, pp. 607–619, 2011.
- [17] T. Kanade, J. F. Cohn, and Y. Tian, “Comprehensive database for facial expression analysis,” in *FG*, 2000, pp. 46–53.
- [18] P. Lucey, J. F. Cohn, T. Kanade, J. Saragih, Z. Ambadar, and I. Matthews, “The extended cohn-kanade dataset (ck+): A complete expression dataset for action unit and emotion-specified expression,” in *CVPR Workshops*, 2010, pp. 94–101.

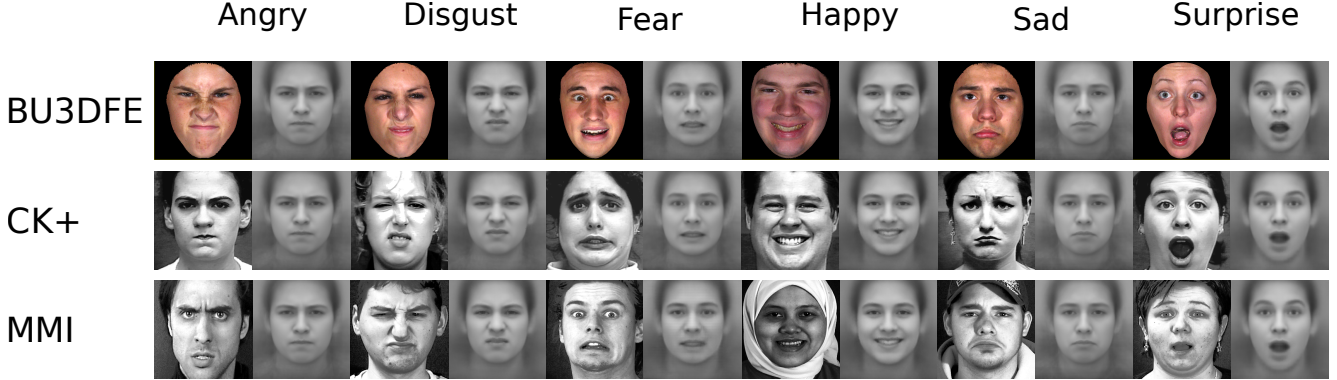


Figure 3: Examples of expression transfer results generated by IF-GAN on the BU-3DFE, CK+, and MMI datasets.

- [19] M. Pantic, M. Valstar, R. Rademaker, and L. Maat, “Web-based database for facial expression analysis,” in *ICME*. IEEE, 2005, pp. 5–pp.
- [20] L. Yin, X. Chen, Y. Sun, T. Worm, and M. Reale, “A high-resolution 3d dynamic facial expression database,” in *FG*. IEEE, 2008, pp. 1–6.
- [21] A. Asthana, S. Zafeiriou, S. Cheng, and M. Pantic, “Robust discriminative response map fitting with constrained local models,” in *CVPR*, 2013, pp. 3444–3451.
- [22] J. Wang, L. Yin, X. Wei, and Y. Sun, “3d facial expression recognition based on primitive surface feature distribution,” in *CVPR*. IEEE, 2006, vol. 2, pp. 1399–1406.
- [23] S. Berretti, A. Del Bimbo, P. Pala, B. Amor, and M. Daoudi, “A set of selected sift features for 3d facial expression recognition,” in *ICPR*. IEEE, 2010, pp. 4125–4128.
- [24] X. Yang, D. Huang, Y. Wang, and L. Chen, “Automatic 3d facial expression recognition using geometric scattering representation,” in *FG Workshops*. IEEE, 2015, vol. 1, pp. 1–6.
- [25] M. Liu, S. Li, S. Shan, R. Wang, and X. Chen, “Deeply learning deformable facial action parts model for dynamic expression analysis,” in *ACCV*. Springer, 2014, pp. 143–157.
- [26] Z. Wang, S. Wang, and Q. Ji, “Capturing complex spatio-temporal relations among facial muscles for facial expression recognition,” in *CVPR*, 2013, pp. 3422–3429.
- [27] E. Sariyanidi, H. Gunes, and A. Cavallaro, “Learning bases of activity for facial expression recognition,” *IEEE T-IP*, vol. 26, no. 4, pp. 1965–1978, 2017.
- [28] S. Jain, C. Hu, and J. Aggarwal, “Facial expression recognition with temporal modeling of shapes,” in *ICCV Workshops*, 2011, pp. 1642–1649.
- [29] A. Sanin, C. Sanderson, M. Harandi, and B. Lovell, “Spatiotemporal covariance descriptors for action and gesture recognition,” in *WACV*, 2013, pp. 103–110.
- [30] M. Liu, S. Shan, R. Wang, and X. Chen, “Learning expressionlets on spatio-temporal manifold for dynamic facial expression recognition,” in *CVPR*, 2014, pp. 1749–1756.
- [31] K. Sikka, G. Sharma, and M. Bartlett, “Lomo: Latent ordinal model for facial analysis in videos,” in *CVPR*, 2016, pp. 5580–5589.
- [32] W. Chu, F. De la Torre, and J. Cohn, “Selective transfer machine for personalized facial expression analysis,” *IEEE T-PAMI*, 2016.
- [33] H. Jung, S. Lee, J. Yim, S. Park, and J. Kim, “Joint fine-tuning in deep neural networks for facial expression recognition,” in *ICCV*, 2015, pp. 2983–2991.
- [34] Y. Lai and S. Lai, “Emotion-preserving representation learning via generative adversarial network for multi-view facial expression recognition,” in *FG*. IEEE, 2018, pp. 263–270.
- [35] F. Zhang, T. Zhang, Q. Mao, and C. Xu, “Joint pose and expression modeling for facial expression recognition,” in *CVPR*, 2018, pp. 3359–3368.
- [36] R. Ptucha, G. Tsagkatakis, and A. Savakis, “Manifold based sparse representation for robust expression recognition without neutral subtraction,” in *ICCV Workshops*, 2011, pp. 2136–2143.
- [37] Y. Wen, K. Zhang, Z. Li, and Y. Qiao, “A discriminative feature learning approach for deep face recognition,” in *ECCV*. Springer, 2016, pp. 499–515.
- [38] H. Ding, S. Zhou, and R. Chellappa, “Facenet2expnet: Regularizing a deep face recognition net for expression recognition,” in *FG*. IEEE, 2017, pp. 118–126.
- [39] A. T. Lopes, E. de Aguiar, A. De Souza, and T. Oliveira-Santos, “Facial expression recognition with convolutional neural networks: coping with few data and the training sample order,” *Pattern Recognition*, vol. 61, pp. 610–628, 2017.
- [40] X. Zhao, X. Liang, L. Liu, T. Li, Y. Han, N. Vasconcelos, and S. Yan, “Peak-piloted deep network for facial expression recognition,” in *ECCV*. Springer, 2016, pp. 425–442.